Bounded dynamics in finite $\mathcal{PT}$-symmetric magnetic metamaterials

Mario I. Molina

Departamento de Física, MSI-Nucleus on Advanced Optics, and Center for Optics and Photonics (CEFOP),
Facultad de Ciencias, Universidad de Chile, Santiago, Chile

We examine the $\mathcal{PT}$-symmetry-breaking transition for a magnetic metamaterial of a finite extent, modeled as an array of coupled split-ring resonators in the equivalent circuit model approximation. Small-size arrays are solved completely in closed form, while for arrays larger than $N = 5$ results were computed numerically for several gain and loss spatial distributions. In all cases, it is found that the parameter stability window decreases rapidly with the size of the array, until at $N = 20$ approximately it is not possible to support a stable $\mathcal{PT}$-symmetric phase.

The study of $\mathcal{PT}$-symmetric systems has attracted a lot of attention during the past few years. In these systems, the effects of loss and gain can balance each other and, as a result, give rise to a bounded dynamics. These studies are based on the seminal work of Bender and coworkers [1,2], who showed that non-Hermitian Hamiltonians are capable of displaying a purely real eigenvalue spectrum provided the system is symmetric with respect to the combined operations of parity ($\mathcal{P}$) and time-reversal ($\mathcal{T}$) symmetry. For one-dimensional systems the $\mathcal{PT}$ requirement leads to the condition that the imaginary part of the potential term in the Hamiltonian be an odd function, while the real part be even. The system thus described can experience a spontaneous symmetry breaking from a $\mathcal{PT}$-symmetric phase (all eigenvalues real) to a broken phase (at least two complex eigenvalues), as the gain and loss parameters are varied. To date, numerous $\mathcal{PT}$-symmetric systems have been explored in several fields, from optics [3–7], electronic circuits [8], solid-state and atomic physics [9,10], to magnetic metamaterials [11], among others. The $\mathcal{PT}$-symmetry-breaking phenomenon has been observed in several experiments [6,7,12].

Magnetic metamaterials, on the other hand, consist of artificial structures whose magnetic response can be tailored to a certain extent. A common realization of such a system consists of an array of metallic split-ring resonators (SRRs) coupled inductively [13–15]. This type of system can feature negative magnetic response in some frequency window, making them attractive for use as a constituent in negative refraction index materials [16]. A common problem with SRRs is the heavy ohmic and radiative losses. One possible solution is to endow the SRRs with external gain, such as tunnel (Esaki) diodes [17,18] to compensate for such losses.

In this work, we consider the $\mathcal{PT}$-symmetry properties of a SRR array endowed with gain and loss. In the case of some one-dimensional coupled discrete systems, such as a harmonic oscillator array, it has been observed that in the limit of an infinite size array, the system belongs to the broken $\mathcal{PT}$ phase, i.e., there are complex eigenvalues making the dynamics unbounded [11,19]. Here we examine the case of short SRRs arrays and determine the parameter window inside which the system exhibits a bounded dynamics and how this window decreases with the size of the system.

The model. Let us consider a very simple model of a magnetic metamaterial consisting of a finite one-dimensional array of SRRs including gain and loss terms. In the equivalent circuit model approach [20], each SRR is equivalent to an RCL circuit with inductance L, capacitance C, and gain and loss R_n. The rings are inductively coupled through magnetic dipole-dipole interactions. The capacitance is given explicitly by $C = \epsilon_o \epsilon A/d$, where ϵ_0 is the permittivity of the vacuum, ϵ is the linear permittivity, A is the area of the cross section of the wire, and d is the size of the slit. The dynamics of charges Q_n and currents I_n are given by

$$\frac{dQ_n}{dt} = I_n, \tag{1}$$

$$L\frac{dI_n}{dt} + R_n I_n + \frac{Q_n}{C} = -M\left(\frac{dI_{n-1}}{dt} + \frac{dI_{n+1}}{dt}\right), \tag{2}$$

where M is the mutual inductance coefficient and where we have assumed coupling to nearest neighbors only. We proceed now to normalize Eq. (2) by defining a set of dimensionless quantities: $q_n = Q_n/Q_c, i_n = I_n/I_c, \tau = \omega t, \gamma_n = R_n C \omega$, and $\lambda = M/L$, where $\omega^{-2} = LC, I_c = U_c \omega C, Q_c = C U_c$, with $U_c = d E_c$, where E_c is a typical value for the electric field in the slit.

In terms of these dimensionless quantities, the evolution equations for the charge q_n of the nth SRR become

$$\frac{d^2}{d\tau^2}[q_n + \lambda(q_{n+1} + q_{n-1})] + \gamma_n \frac{d}{d\tau}q_n + q_n = 0, \tag{3}$$

where λ is the magnetic interaction coefficient or coupling, and γ_n positive (negative) denotes a ring with loss (gain). For simplicity, in Eq. (3) we assume the absence of nonlinear effects and the relative orientations of the SRRs is chosen such that the electric coupling among SRRs can be neglected. In order to satisfy the requirements for $\mathcal{PT}$ symmetry, the spatial distributions of the gain and loss must be an odd function in space [3], $\gamma_{-n} = -\gamma_n$. In this work we focus on binary-like systems with two gain and loss terms and thus examine arrays of the form $\ldots -\gamma_1,-\gamma_2,-\gamma_1,0,\gamma_1,\gamma_2,\gamma_1,\ldots,$ for arrays with an odd number of rings. For arrays with even number of rings the distribution of gain and loss is of the form $\ldots -\gamma_1,-\gamma_2,-\gamma_1,\gamma_1,\gamma_2,\gamma_1,\ldots.$ This distinction is only meaningful for small arrays and disappears for systems of infinite size. Hereafter, and without loss of generality, we focus on arrays with an odd number of sites (except for the

dimer case). Results for the case with an even number of sites are similar. Since the values of γ_1 and γ_2 are arbitrary, the gain and loss distribution thus introduced allows for many interesting cases to be examined. In particular we focus on three cases. The first one is $\gamma_1 = \gamma$, $\gamma_2 = -\gamma$, giving rise to the distribution $\ldots \gamma, -\gamma, \gamma, -\gamma, 0, \gamma, -\gamma, \gamma, -\gamma \ldots$. The second one is $\gamma_1 = \gamma$ and $\gamma_2 = 0$, which gives rise to the distribution $\ldots 0, -\gamma, 0, -\gamma, 0, \gamma, 0, \gamma, 0, \ldots$. Another interesting case is the one with $\gamma_1 = \gamma = \gamma_2$ that gives $\ldots -\gamma, -\gamma, -\gamma, -\gamma, 0, \gamma, \gamma, \gamma, \gamma \ldots$. For this last case, we will see that in spite of the concentration of loss and gain on opposite sides, the dynamics does possess a stability window for finite arrays lengths.

Dimer case (N = 2). In this case, the only possible case is $\gamma, -\gamma$. The dynamical equations read

$$\frac{d^2}{d\tau^2}(q_1 + \lambda q_2) + \gamma \frac{d}{d\tau} q_1 + q_1 = 0, \tag{4}$$

$$\frac{d^2}{d\tau^2}(q_2 + \lambda q_1) - \gamma \frac{d}{d\tau} q_2 + q_2 = 0. \tag{5}$$

We look for stationary modes $q_{1,2}(\tau) = q_{1,2} \exp(i\Omega\tau)$. This leads to the equations

$$-\Omega^2(q_1 + \lambda q_2) + i\gamma\Omega q_1 + q_1 = 0, \tag{6}$$

$$-\Omega^2(q_2 + \lambda q_1) - i\gamma\Omega q_2 + q_2 = 0. \tag{7}$$

The condition of the vanishing of the determinant of this linear system leads to a quadratic equation for Ω^2, with solutions

$$\Omega = \pm \left[\frac{2 - \gamma^2 \pm \sqrt{\gamma^4 - 4\gamma^2 + 4\lambda^2}}{2(1 - \lambda^2)} \right]^{1/2}. \tag{8}$$

We denote the four solutions as $\Omega^{++}, \Omega^{+-}, \Omega^{-+}$, and Ω^{--}. The stable phase (unbroken $\mathcal{PT}$ symmetry) corresponds to the cases where Ω is a real quantity. From straightforward examination of Eq. (6), one concludes that the stability window in γ-λ space is given by the area under the curve $\gamma_c = \sqrt{2(1 - \sqrt{1 - \lambda^2})}$, for $0 < \lambda < 1$. Outside $\gamma = \gamma_c(\lambda)$, the system is unstable. Figure 1 shows the stability region and also the square frequencies as a function of the gain and loss parameter. Due to symmetry considerations, only the positive γ-λ sector needs to be explored.

From Eq. (4) [or Eq. (5)] and Eq. (6), it is easy to obtain $|q_2/q_1| = 1$ and thus, q_1 and q_2 differ by a phase only. We

FIG. 2. (Color online) Dimer array. Mode phase as a function of the gain and loss parameter. Solid: Ω^{++} mode. Dotted: Ω^{+-} mode. Short dash: Ω^{--} mode. Long dash: Ω^{-+} mode. ($\lambda = 0.33$).

have four branches for the phase, corresponding to each of the four solutions. Figure 2 shows the phase of all solutions as a function of the gain and loss parameter.

Trimer case (N = 3). Here the gain and loss distribution has the form $-\gamma, 0, \gamma$. The stationary state equations have the form

$$-\Omega^2(q_1 + \lambda q_2) + i\gamma\Omega q_1 + q_1 = 0, \tag{9}$$

$$-\Omega^2(q_2 + \lambda(q_2 + q_3)) + q_2 = 0, \tag{10}$$

$$-\Omega^2(q_3 + \lambda q_2) - i\gamma\Omega q_3 + q_3 = 0, \tag{11}$$

with eigenvalues

$$\Omega = \pm 1, \tag{12}$$

$$\Omega = \pm \left[\frac{2 - \gamma^2 \pm \sqrt{-4\gamma^2 + \gamma^4 + 8\lambda^2}}{2 - 4\lambda^2} \right]^{1/2}. \tag{13}$$

The condition that *all* Ω be real leads to the conditions $\lambda < 1/\sqrt{2}$ and $\gamma < \gamma_c = \sqrt{2 - \sqrt{4 - 8\lambda^2}}$. Figure 3 shows the window of real eigenvalues in gain and loss coupling space. It is qualitatively similar to the dimer case, but the allowed coupling interval is smaller. The figure also shows the square of the real frequency as a function of gain and loss, for a given coupling value.

Pentamer case (N = 5). Here the gain and loss distribution can have three possible forms: $\gamma, -\gamma, 0, \gamma, -\gamma$, or $0, -\gamma, 0, \gamma, 0$, or $-\gamma, -\gamma, 0, \gamma, +\gamma$. We focus on the first case since is more amenable to an exact form solution (numerical
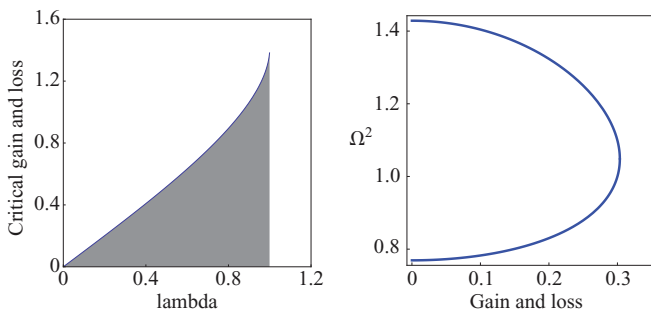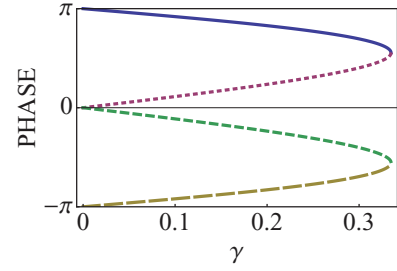

FIG. 1. (Color online) Dimer array. Left: Stability region (shaded) in gain and loss-coupling space. Right: Mode frequency squared as a function of the gain and loss parameter for $\lambda = 0.3$.
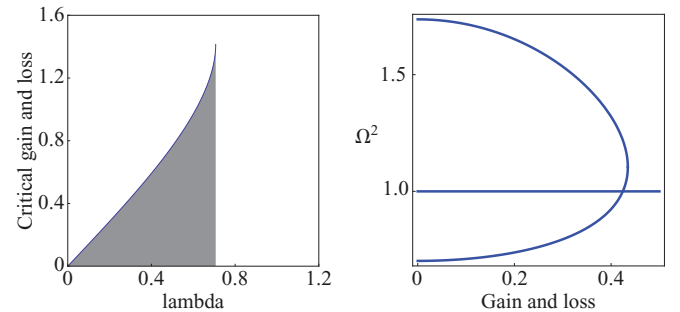

FIG. 3. (Color online) Trimer array. Left: Stability region (shaded) in gain and loss coupling space. Right: Mode frequency squared as a function of the gain and loss parameter, for $\lambda = 0.3$.

results show that the other two cases display similar behavior). The stationary state equations have the form

$$-\Omega^2(q_1 + \lambda q_2) + i\gamma\Omega q_1 + q_1 = 0, \tag{14}$$

$$-\Omega^2(q_2 + \lambda(q_1 + q_3)) - i\gamma\Omega q_2 + q_2 = 0, \tag{15}$$

$$-\Omega^2(q_3 + \lambda(q_2 + q_4)) + q_3 = 0, \tag{16}$$

$$-\Omega^2(q_4 + \lambda(q_3 + q_5)) + i\gamma\Omega q_4 + q_4 = 0, \tag{17}$$

$$-\Omega^2(q_5 + \lambda q_4) - i\gamma\Omega q_5 + q_5 = 0, \tag{18}$$

with eigenvalues

$$\Omega = \pm 1, \tag{19}$$

$$\Omega = \pm\left[\frac{2 - \gamma^2 \pm \sqrt{-4\gamma^2 + \gamma^4 + 4\lambda^2}}{2 - 2\lambda^2}\right]^{1/2}, \tag{20}$$

$$\Omega = \pm\left[\frac{2 - \gamma^2 \pm \sqrt{-4\gamma^2 + \gamma^4 + 12\lambda^2}}{2 - 6\lambda^2}\right]^{1/2}. \tag{21}$$

The condition that *all* Ω be real leads to the conditions $\lambda < 1/\sqrt{3}$ and $\gamma < \gamma_c = \sqrt{2(1 - \sqrt{1 - \lambda^2})}$. Figure 4 shows the stability window in gain and loss coupling space, as well as the square frequency as a function of gain and loss, for a fixed coupling value. As we can see, the stability window is substantially smaller than the one for the dimer and trimer cases.

Short chains (N > 5). Let us consider now the case of finite arrays, where the stationary-state equations are given by

$$-\Omega^2[q_n + \lambda(q_{n+1} + q_{n-1})] + (1 + i\Omega\gamma_n)q_n = 0. \tag{22}$$

The $\{\gamma_n\}$ distribution we consider has the general form $\ldots, -\gamma_1, -\gamma_2, -\gamma_1, 0, \gamma_1, \gamma_2, \gamma_1, \ldots$. We compute the relevant eigenvalues numerically from the vanishing of the determinant of linear system (22) and focus on the parameter values in gain and loss coupling space where the eigenvalues are purely real, thus denoting a bounded dynamical regime.

Case a. We start with the case $\gamma_1 = -\gamma_2 \equiv \gamma$ that gives rise to the distribution $\ldots, -\gamma, +\gamma, -\gamma, 0, +\gamma, -\gamma, +\gamma, \ldots$. Some results are shown in Fig. 5. It is clear that as the size of the array increases, the stability region shrinks, and it disappears altogether around $N = 20$. This is consistent with a previous
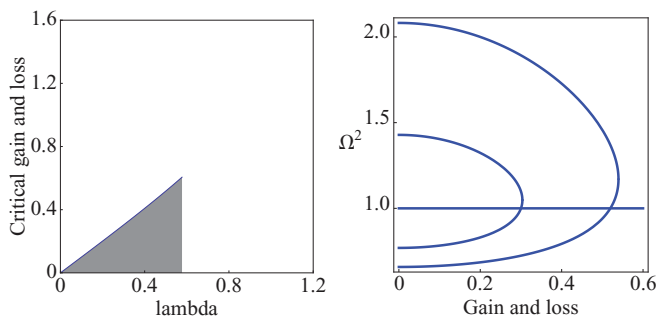

FIG. 5. Stability regions (area under curve) in gain and loss coupling space for several array lengths, for the case $\ldots, -\gamma, +\gamma, -\gamma, 0, +\gamma, -\gamma, +\gamma, \ldots$.

result [11] stating that in the infinity size limit, the dynamics is always unstable (that is, the system belongs to the broken $\mathcal{PT}$ phase).

Case b. Now we take $\gamma_2 \to 0$ and $\gamma_1 \equiv \gamma$, that is, the distribution $\ldots, 0, -\gamma, 0, -\gamma, 0, +\gamma, 0, +\gamma, 0, +\gamma, 0, \ldots$. Notice how the gain and loss portions are now separated and on each side they are rather diluted. The stability phase diagrams for this case (not shown) are qualitatively similar to the previous case, although, for a given array size, the stability windows are smaller.

Case c. Now we take $\gamma_2 = \gamma_1 \equiv \gamma$. The gain and loss distribution is $\ldots, -\gamma, -\gamma, -\gamma, -\gamma, 0, +\gamma, +\gamma, +\gamma, +\gamma, \ldots$. Now the gain and loss on each side are densely populated and the resulting area of the stability windows (not shown) while qualitatively similar to the previous cases, drop even faster.

Figure 6 shows a summary of the results obtained for the size of the stability window as a function of the array length, for the three cases considered. We clearly see that the stability region decreases rather abruptly with N, and that for a given N, we have area $a <$ area $b <$ area c, for $N > 5$.

The above results can be qualitatively explained by means of a simple estimate of the time needed for magnetic energy to transfer from one ring with gain to a neighboring ring, compared to the time employed by the ring to accumulate energy. For a large array, and in the absence of gain and loss effects, we have the dispersion relation for the magnetoinductive waves: $\Omega_k = [1 - 2\lambda\cos(k)]^{-1/2}$. The group velocity of these waves will be $v_k = d\Omega_k/dk$, that is,

$$v_k = \lambda\frac{\sin(k)}{[1 - 2\lambda\cos(k)]^{3/2}}. \tag{23}$$

For a ring with gain, the amplitude grows in time as $\exp(\gamma\tau)$; therefore, in order for a wave with wave vector k to be stable, its

FIG. 4. (Color online) Pentamer array. Left: Stability region (shaded) in gain and loss coupling space. Right: Mode frequency squared as a function of the gain and loss parameter, for $\lambda = 0.3$.
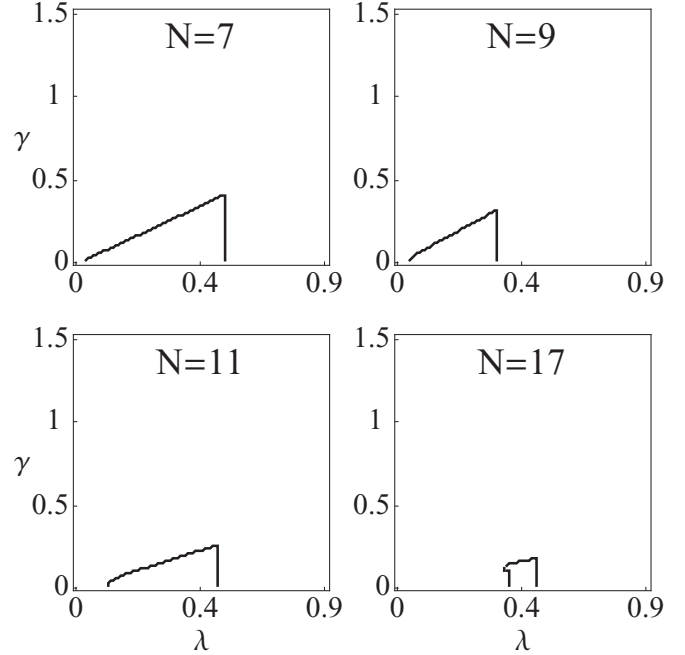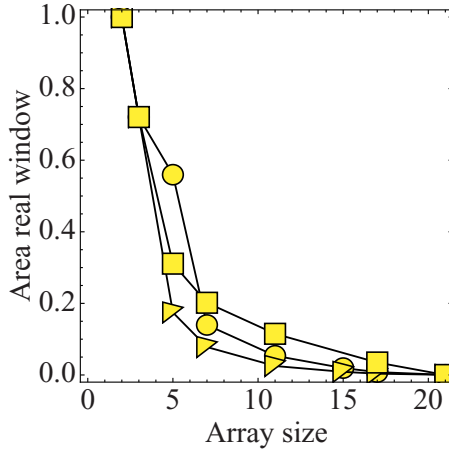
FIG. 6. (Color online) Normalized size of area in gain and loss coupling space with purely real eigenvalues as a function of array size for the gain and loss distributions "a" (squares), "b" (circles), and "c" (triangles).

velocity v_k needs to be greater than the speed at which the ring accumulates energy: $v_k > \gamma$. In order for the whole system to be stable, one needs this to hold for every k. In particular, for the slowest modes, $k \ll 1$, one has for a periodic array, $k = \pi/(N-1)$. This implies

$$\gamma < \frac{\lambda}{(N-1)(1-2\lambda)^{3/2}}, \tag{24}$$

defining a critical gain and loss parameter value that decreases steadily as $1/N$ as N increases. Thus, in the infinite lattice limit, the system will always be in the broken $\mathcal{PT}$ phase. A

physical interpretation follows: In a large array there is no time for the accumulated energy to be transferred away from one gain site to neighboring sites, thus causing the instability.

Conclusions. We have examined finite, one-dimensional $\mathcal{PT}$-symmetric arrays of split-ring resonators, that constitute the simplest model of a magnetic metamaterial, and have focused on the conditions in parameter space where a $\mathcal{PT}$-symmetric phase is stable, i.e., all eigenvalues are real. The dimer, trimer, and pentamer cases were solved in closed form, while for larger but finite arrays, results were obtained numerically. It was found that, for all gain and loss distributions examined, the stability region in parameter space decreases rapidly with an increase in system size, until it disappears altogether at approximately $N = 20$. A simple argument shows a general tendency of a coupled system to increase its instability window as its size increases. This tendency seems generic for gain and loss distributions based on two gain and loss parameters and is consistent with recent results for infinite discrete arrays [11,19]. We believe that the relatively small size of the structures at which $\mathcal{PT}$ symmetry is broken, together with the availability of negative resistance devices for providing gain [18], greatly facilitates the experimental study of this transition.

The study of the robustness of the results reported here under the inclusion of effects such as the electric coupling among the SRRs and nonlinear effects is under way and will be reported elsewhere.

[1] C. M. Bender and S. Boettcher, Phys. Rev. Lett. **80**, 5243 (1998).

[2] C. M. Bender, D. C. Brody, and H. F. Jones, Phys. Rev. Lett. **89**, 270401 (2002).

[3] R. El-Ganainy, K. G. Makris, D. N. Christodoulides, and Z. H. Musslimani, Opt. Lett. **32**, 2632 (2007).

[4] Z. H. Musslimani, K. G. Makris, R. El-Ganainy, and D. N. Christodoulides, Phys. Rev. Lett. **100**, 030402 (2008).

[5] K. G. Makris, R. El-Ganainy, D. N. Christodoulides, and Z. H. Musslimani, Phys. Rev. Lett. **100**, 103904 (2008).

[6] A. Guo, G. J. Salamo, D. Duchesne, R. Morandotti, M. Volatier-Ravat, V. Aimez, G. A. Siviloglou, and D. N. Christodoulides, Phys. Rev. Lett. **103**, 093902 (2009).

[7] C. E. Rüter, K. G. Makris, R. El-Ganainy, D. N. Christodoulides, M. Segev, and D. Kip, Nat. Phys. **6**, 192 (2010).

[8] J. Schindler, Ang Li, M. C. Zheng, F. M. Ellis, and T. Kottos, Phys. Rev. A **84**, 040101(R) (2011).

[9] N. Hatano and D. R. Nelson, Phys. Rev. Lett. **77**, 570 (1996).

[10] Y. N. Joglekar, D. Scott, M. Babbey, and Avadh Saxena, Phys. Rev. A **82**, 030103 (2010).

[11] N. Lazarides and G. P. Tsironis, Phys. Rev. Lett. **110**, 053901 (2013).

[12] A. Szameit, M. C. Rechtsman, O. Bahat-Treidel, and M. Segev, Phys. Rev. A **84**, 021806(R) (2011).

[13] T. J. Yen, W. J. Padilla, N. Fang, D. C. Vier, D. R. Smith, J. B. Pendry, D. N. Basov, and X. Zhang, Science **303**, 1494 (2004).

[14] N. Katsarakis, G. Constantinidis, A. Kostopoulos, R. S. Penciu, T. F. Gundogdu, M. Kafesaki, E. N. Economou, Th. Koschny, and C. M. Soukoulis, Opt. Lett. **30**, 1348 (2005).

[15] M. I. Molina, N. Lazarides, and G. P. Tsironis, Phys. Rev. E **80**, 046605 (2009).

[16] R. A. Shelby, D. R. Smith, and S. Schultz, Science **292**, 77 (2001).

[17] L. Esaki, Phys. Rev. **109**, 603 (1958).

[18] T. Jiang, K. Chang, L.-M. Si, L. Ran, and H. Xin, Phys. Rev. Lett. **107**, 205503 (2011).

[19] D. E. Pelinovsky, P. G. Kevrekidis, and D. J. Frantzeskakis, arXiv:1211.5815.

[20] N. N. Rosanov, N. V. Vysotina, A. N. Shatsev, I. V. Shadrivov, D. A. Powell, and Y. S. Kivshar, Opt. Express **19**, 26500 (2011).